

Electronic Supplementary Information

Size-optimized galactose-capped gold nanoparticles for the colorimetric detection of heat-labile enterotoxin at nanomolar concentrations

Vivek Poonthiyil,^{a,b} Vladimir B. Golovko,^{*a,b} and Antony J. Fairbanks^{*a}

^a *Department of Chemistry, University of Canterbury, Private Bag 4800, Christchurch, New Zealand*

^b *The Macdiarmid Institute for Advanced Materials and Nanotechnology, Wellington, 6140, New Zealand.*

E-mail: vladimir.golovko@canterbury.ac.nz, antony.fairbanks@canterbury.ac.nz

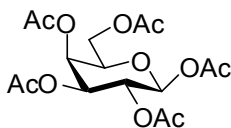
General Experimental

All chemical reagents were of analytical grade and used as supplied without further purification unless otherwise stated. Solvent was removed under reduced pressure using a BuchiTM rotary evaporator. Thin Layer Chromatography (t.l.c.) was carried out on Merck Silica Gel 60F₂₅₄ aluminium backed plates. Plate visualisation was achieved using a UV lamp ($\lambda_{\text{max}} = 254$ or 365 nm), and/or ammonium molybdate (5% in 2M H₂SO₄). Flash column chromatography was carried out using Sorbsil C60 40/60 silica.

Melting points were recorded on an Electrothermal[®] melting point apparatus. Proton and carbon nuclear magnetic resonance (δ_{H} , δ_{C}) spectra were recorded on Bruker AV400 (400MHz), and Bruker AV500 (500MHz) spectrometers. All chemical shifts are quoted on the δ -scale in ppm using residual solvent as an internal standard. High resolution mass spectra were recorded a Bruker FT-ICR mass spectrometer using electrospray ionisation (ESI) or chemical ionisation (CI) techniques as stated. M/z values are reported in Daltons. Optical rotations were measured on a Perkin-Elmer 241 polarimeter with a water-jacketed 1 cm³ cell with a path length of 1 dm, and are quoted in units of $^{\circ} \cdot \text{cm}^2 \cdot \text{g}^{-1}$.

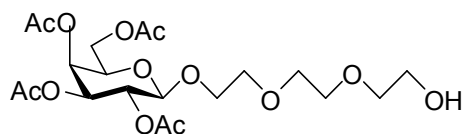
Synthesis of the thiol-terminated galactose ligand.

1,2,3,4,6-Penta-*O*-acetyl- β -D-galactopyranose^{1,2}



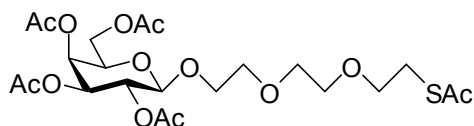
Sodium acetate (41 g, 500 mmol) was added to acetic anhydride (315 mL), and the mixture was refluxed at 120 °C for 30 min. D-Galactose **5** (30.0 g, 165 mmol) was then added slowly over 30 min. After a further 120 min, t.l.c (petrol:ethyl acetate, 1 : 1) showed complete consumption of starting material (R_f 0) and the formation of single product (R_f 0.7). The reaction mixture was then cooled to rt and a mixture of water and ice (400 mL) was added. The ensuing precipitate was filtered, and then recrystallized (ethanol) to give pentaacetate **1** (20.0 g, 31%) as white crystalline solid; m.p. 135-138 °C [lit. m.p. 137-139 °C]¹; $[\alpha]_{\text{D}}^{20} +29.3$ (c , 1.0 in CHCl₃)² [lit. $[\alpha]_{\text{D}}^{23.5} +27.1$ (c , 1.03 in CHCl₃)]; δ_{H} (500 MHz, CDCl₃)³ 1.99, 2.04, 2.11, 2.16 (15H, 4 x s, 5 x CH₃CO₂), 4.07 (1H, m, H-5), 4.13-4.16 (2H, m, H-6, H-6'), 5.06 (1H, dd, $J_{3,4}$ 3.5 Hz, H-3), 5.32 (1H, dd, $J_{2,3}$ 10.5 Hz, H-2), 5.42 (1H, m, H-4), 5.69 (1H, d, $J_{1,2}$ 8.3 Hz, H-1).

8-Hydroxy-3,6-dioxa-octyl 2,3,4,6-tetra-*O*-acetyl- β -D-galactopyranoside 2⁴



BF₃.Et₂O (1.9 mL, 15.4 mmol) was added to a solution of compound **1** (3.0 g, 7.7 mmol) and triethylene glycol (2.2 mL, 17 mmol) in dry DCM (30 mL) and the resulting solution was stirred at room temperature for 5 h. The solution was then diluted with DCM (30 mL) and washed successively with saturated aqueous NaHCO₃ (2 × 30 mL), H₂O (2 × 30 mL), and brine (30 mL). The organic extracts were dried (Na₂SO₄), filtered, and concentrated *in vacuo*. The residue was then purified by flash chromatography (petrol:ethyl acetate, 1:1) to afford alcohol **2** (1.5 g, 40 %) as a yellow syrup; [α]_D²⁰ + 0.3 (c, 1.0 in MeOH); δ _H (400 MHz, CDCl₃)⁴³ 2.15, 2.06, 2.04, 1.98 (12H, 4 x s, 4 x CH₃), 3.77-3.59 (10H, m, 5 x O-CH₂-), 3.95 (2H, m, 1 x CH₂-O), 4.15 (3H, m, H-5, H-6, H-6'), 4.58 (1H, d, *J*_{1,2} 7.8 Hz, H-1), 5.02 (1H, dd, *J*_{3,4} 2.1 Hz, H-3), 5.19 (1H, dd, *J*_{1,2} 7.8 Hz, *J*_{2,3} 8.7 Hz, H-2), 5.38 (1H, m, H-4); HRMS (ESI) Calcd. For C₂₀H₃₃O₁₃ (MH⁺) 481.1916. Found 481.1914;

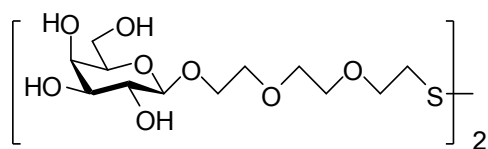
8-Thioacetyl-3,6-dioxa-octyl 2,3,4,6-tetra-*O*-acetyl- β -D-galactopyranoside 3⁴



Triethylene glycol galactoside **7** (2.5 g, 5.3 mmol) was dissolved in dry DCM (100 mL) under nitrogen at 0 °C and stirred. Mesyl chloride (0.7 mL, 10 mmol) was added dropwise, and then triethylamine (1.4 mL, 10 mmol) was added. The reaction mixture was then allowed to warm to room temperature. After 2h, t.l.c (EtOAc) indicated the formation of a single product (R_f 0.3) and the complete consumption of the starting material (R_f 0). The reaction was quenched by the addition of methanol (10 mL) and concentrated *in vacuo*. The residue was dissolved in DMF (25 mL), and potassium thioacetate (2 g, 20 mmol) was added and the reaction was then stirred at 65 °C. After 16 h, t.l.c. (EtOAc) indicated the formation of a major product (R_f 0.4) and the complete consumption of the starting material (R_f 0.3). The reaction mixture was cooled, diluted with EtOAc (30 mL) and washed successively with aqueous NaHCO₃ (2 × 30 mL of a saturated solution), H₂O (2 × 30 mL), and brine (30 mL). The organic layer was separated, dried (Na₂SO₄), filtered, and concentrated *in vacuo*. The residue was purified by flash chromatography

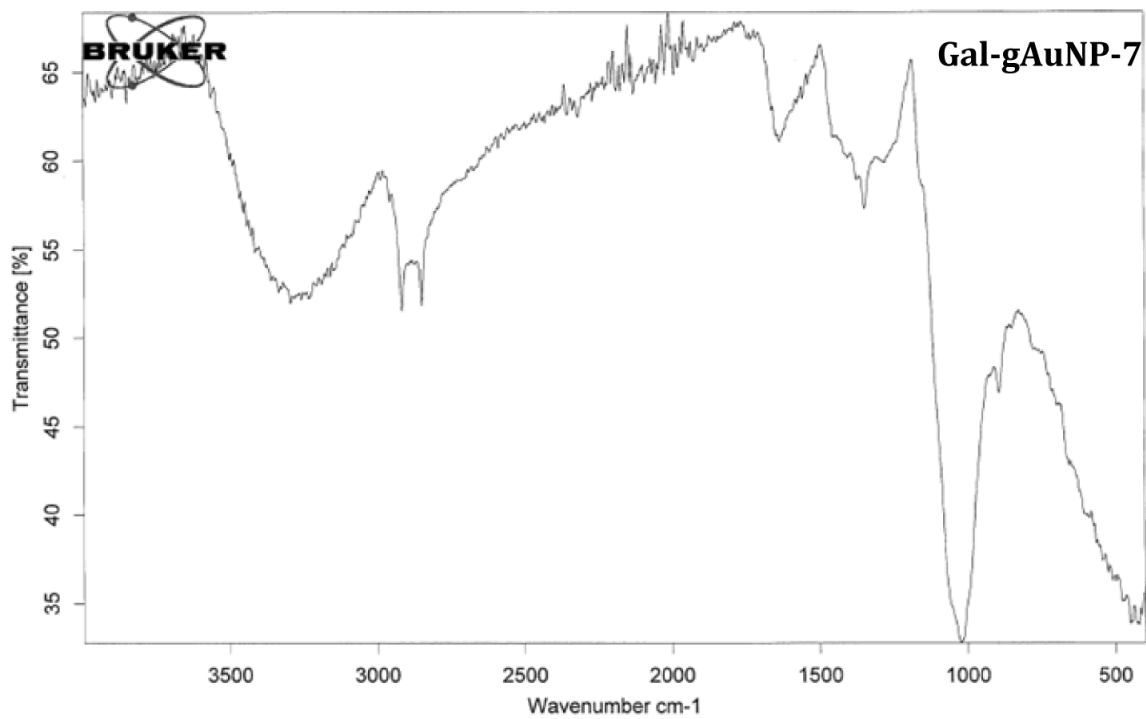
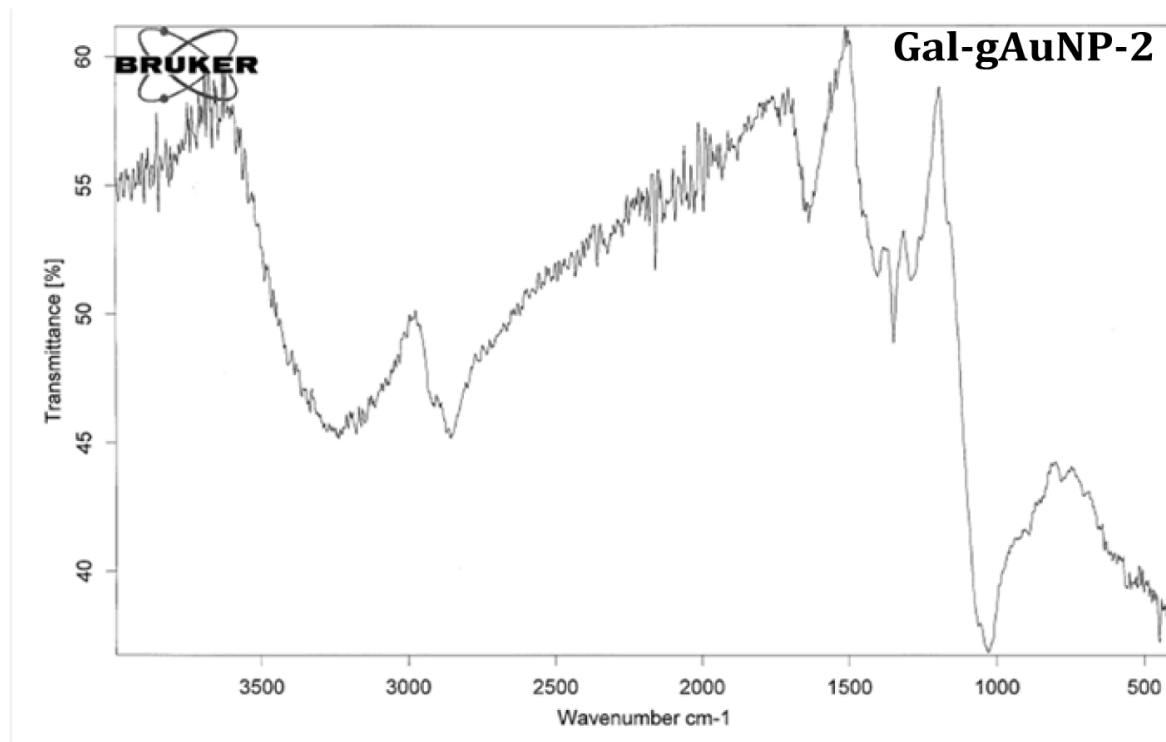
(petrol:EtOAc, 1:3) to afford 8-thioacetyl-3,6-dioxaoctyl 2,3,4,6-tetra-*O*-acetyl- β -D-galactopyranoside **8** (1.9 g, 64.5 %) as a yellow syrup. $[\alpha]_D^{20}$ -3.0 (*c*, 1.0 in CHCl₃); δ_H (400 MHz, CDCl₃)⁴³ 2.14, 2.06, 2.04, 1.98 (12H, 4 x s, 4 x CH₃CO₂), 2.34 (3H, s, 1 x CH₃COS), 3.09 (2H, t, 2 x CH₂SH), 3.58-3.75 (8H, m, 4 x CH₂O), 3.92 (2H, m, 1 x CH₂-O), 4.14 (3H, m, H-5, H-6, H-6'), 4.57 (1H, d, *J*_{1,2} 7.8 Hz, H-1), 5.02 (1H, dd, *J*_{3,4} 2.1 Hz, H-3), 5.21 (1H, dd, *J*_{2,1} 7.8 Hz, *J*_{2,3} 8.7 Hz, H-2), 5.39 (1H, m, H-4); HRMS (ESI) Calcd. For C₂₂H₃₄O₁₃SNa(MNa⁺) 561.1612. Found 561.1617.

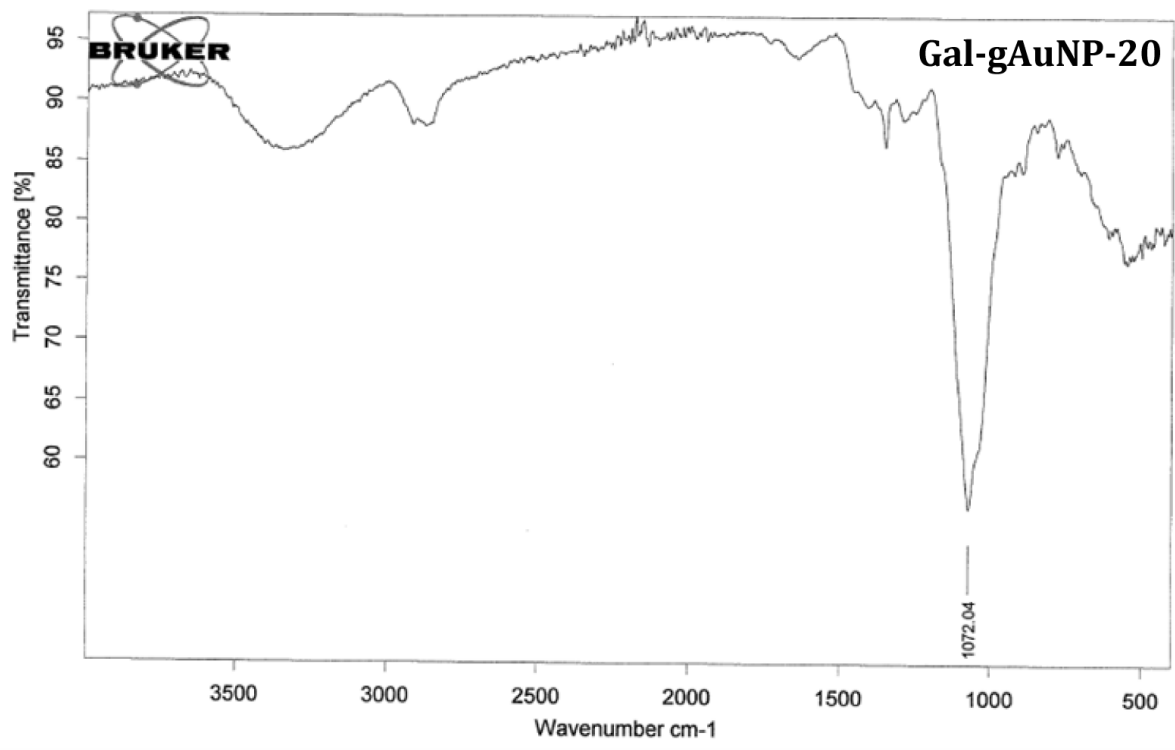
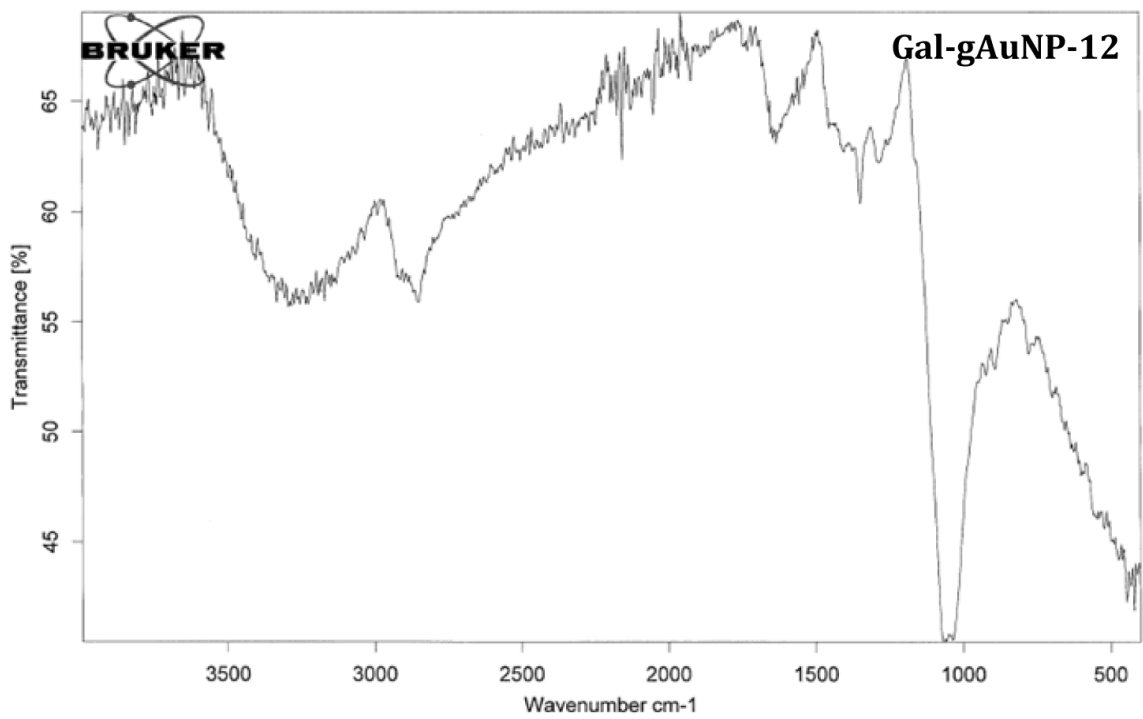
8,8'-Dithiobis(3,6-dioxaoctyl- β -D-galactopyranoside) **4**⁴



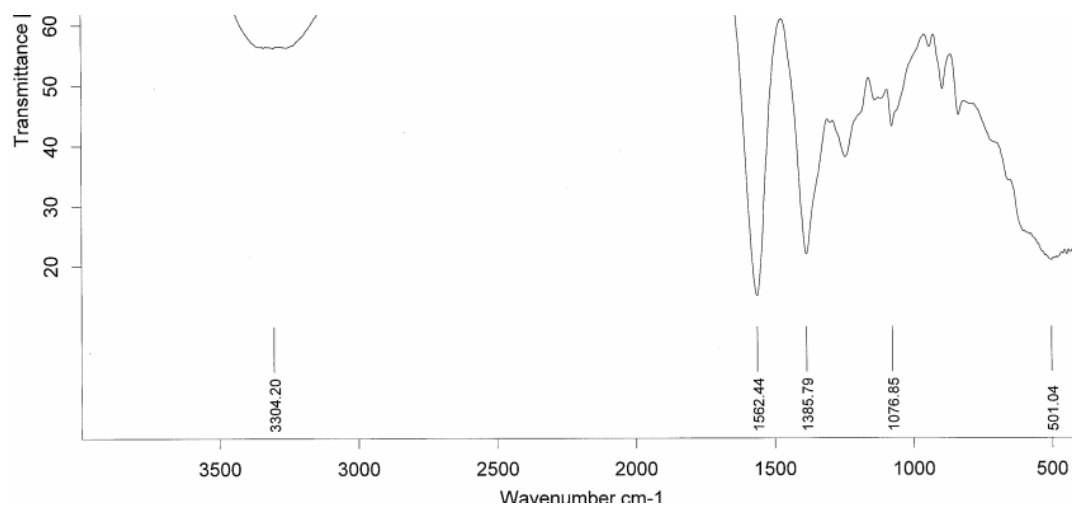
NaOMe (0.17 M in MeOH, 1 mL) was added to a solution of compound **3** (500 mg, 0.93 mmol) in MeOH (10 mL), and the solution was stirred at room temperature for 2 h. The solution was then neutralized by the addition of Amberlite IR-120 (H⁺ resin), filtered, and then air oxidized by bubbling air continuously through the solution for a total of 64 h. The solvent was then removed *in vacuo* to afford disulfide **4** (295 mg, 97 %) as a yellow syrup. $[\alpha]_D^{20}$ -1.6 (*c*, 1.0 in D₂O); δ_H (500 MHz, d₆-DMSO)⁴³ 2.81 (2H, t, CH₂-S-), 3.40 (1H, m, H-2), 3.48-3.65 (10H, m, 4 x CH₂-O, H-6, H-6'), 3.69 (3H, m, 1 x CH₂-O, H-4), 3.77 (1H, m, H-3), 3.93 (1H, m, H-5), 4.28 (1H, d, *J*_{1,2} 8.5 Hz, H-1); HRMS (ESI) Calcd. For C₂₄H₄₆O₁₆S₂(MNa⁺) 677.2119. Found 677.2110

FT-IR spectra of Gal-gAuNPs

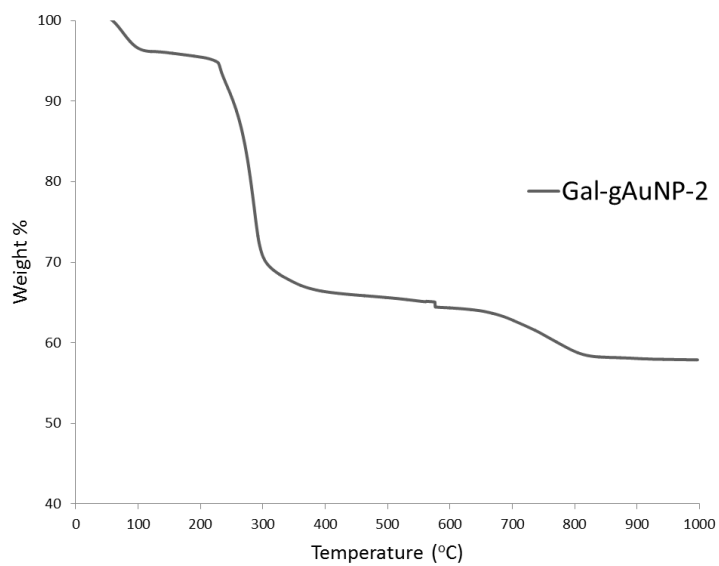


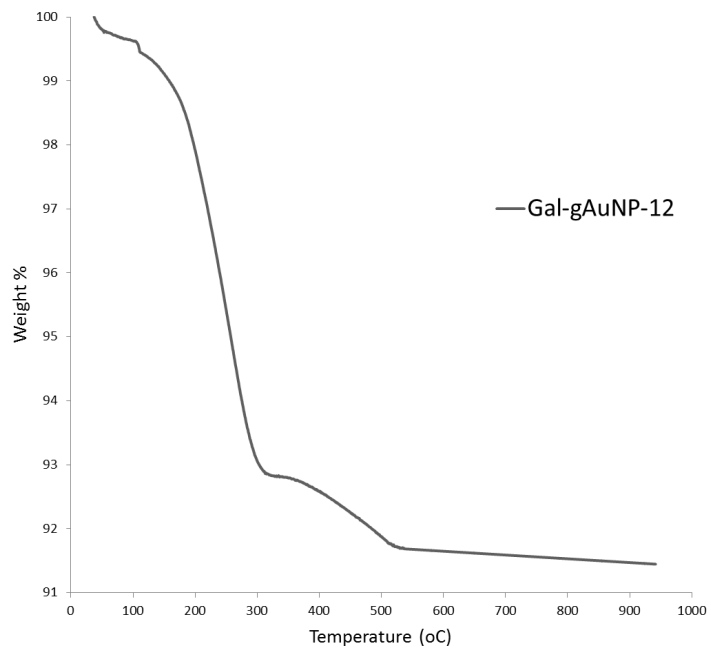
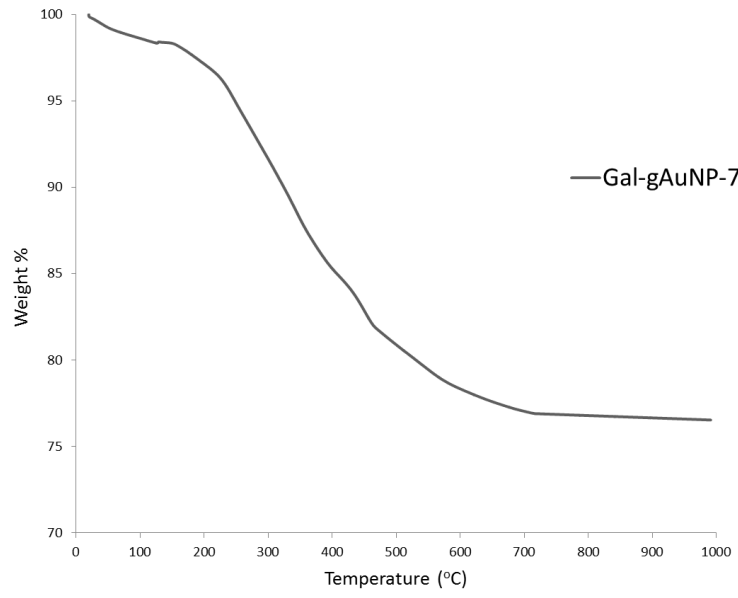


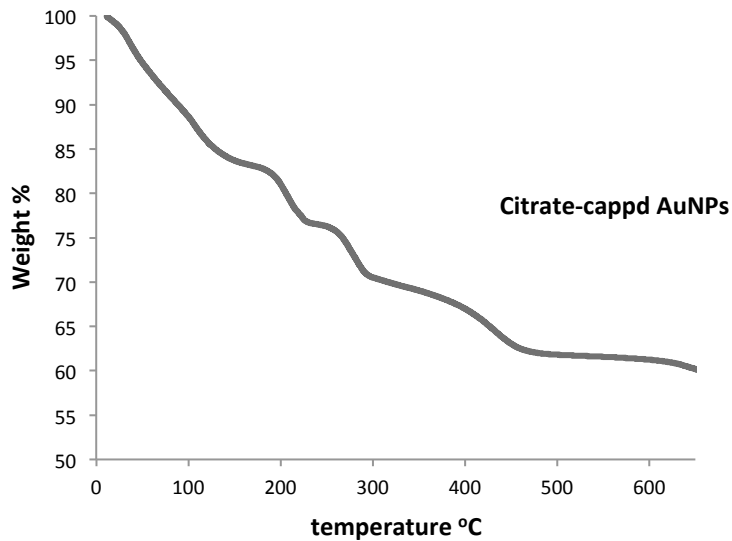
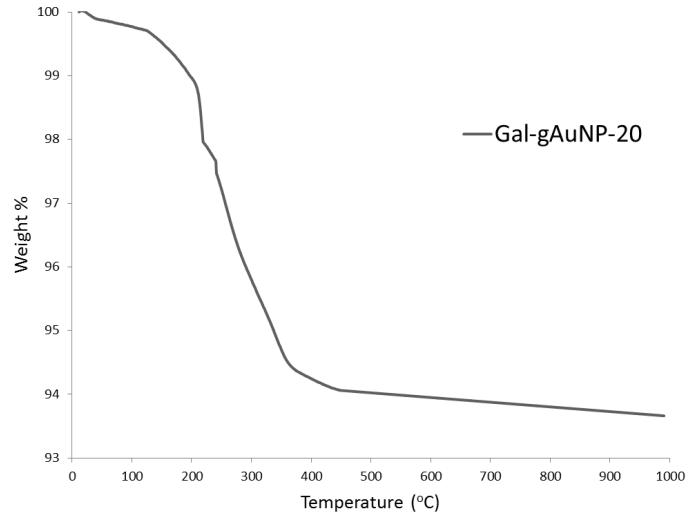
FT-IR spectra of citrate-stabilized AuNPs



TGA plots of Gal-gAuNPs







Calculation of the number of Au atoms and the thiolated ligands per NP

The number of Au atoms (N_{Au}) and the number of thiolate ligands (N_L) per nanoparticles was calculated according to the following equation:

$$N_{Au} = \frac{V_{NP} \times APF}{V_{Au}} = \frac{4\pi \frac{r_{NP}^3}{3} \times 0.7405}{4\pi r_{Au}^3 / 3} = \frac{\left(\frac{d_{NP}}{2}\right)^3 \times 0.7405}{0.144^3} = d_{NP}^3 \times 31$$

$$m_{Au} = N_{Au} \times 196.97$$

$$m_L = m_{Au} \times (\text{wt\% of L} / \text{wt\% of Au})$$

$$N_L = m_L / M_L$$

For N_{Au} , V_{NP} is the volume of a spherical gold NP, V_{Au} is the volume of a gold atom, APF is atomic packing factor, r_{NP} and d_{NP} are the radius and the diameter of a gold NP, and r_{Au} is the radius of a Au atom. m_{Au} , m_L , and M_L are the mass of the gold atoms in the NP, mass of the ligands in the NP, and the molecular mass of the ligand respectively. The wt% of the ligand (L) and wt% of Au are obtained from TGA.

Particle size distributions of Gal-gAuNPs

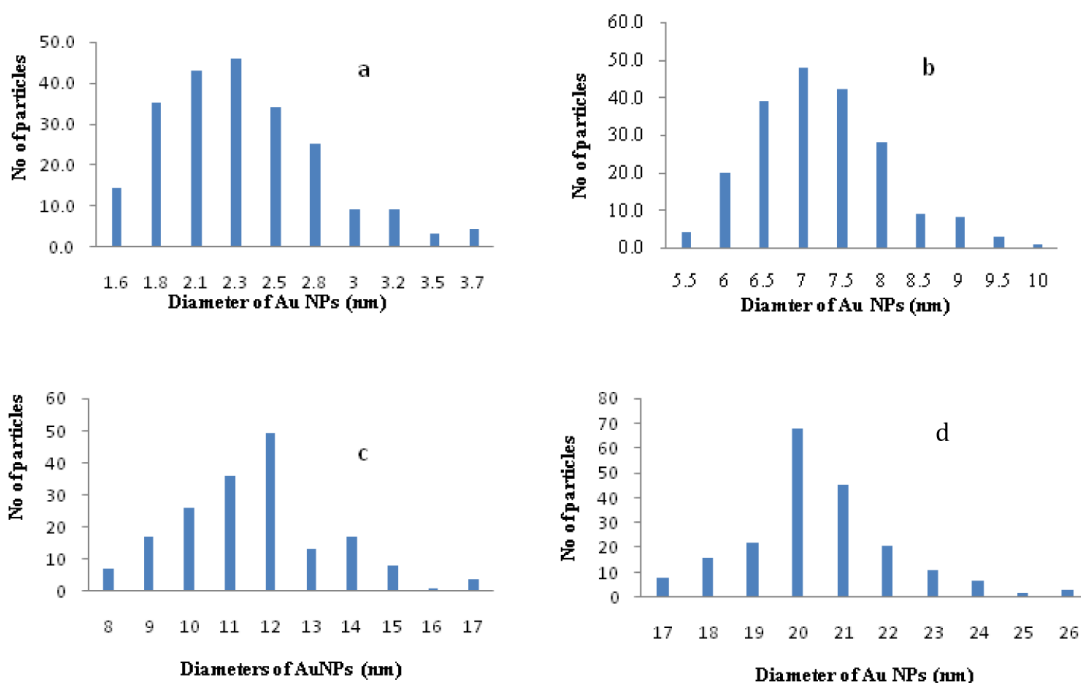


Fig S1. Size distribution histograms of a) Gal-gAuNP-2, b) Gal-gAuNP-7, c) Gal-gAuNP-12, and (d) Gal-gAuNP-20. At least 200 Au NPs were measured for the statistics of particle size distributions in all cases.

Length of the thiol-modified ligand length

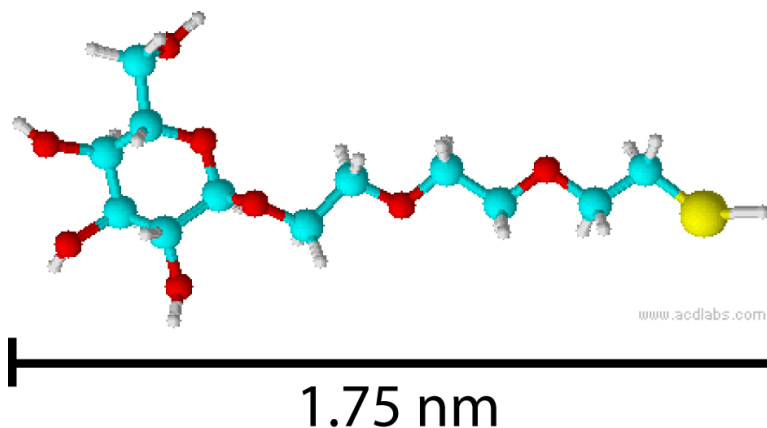


Fig. S2 Thiol-terminated galactose ligand assuming an extended conformation for the triethylene glycol linker and a 4C_1 conformation for galactose

A putative geometry-based hypothesis for the size effect of sensing of LTB by the Gal-gAuNPs

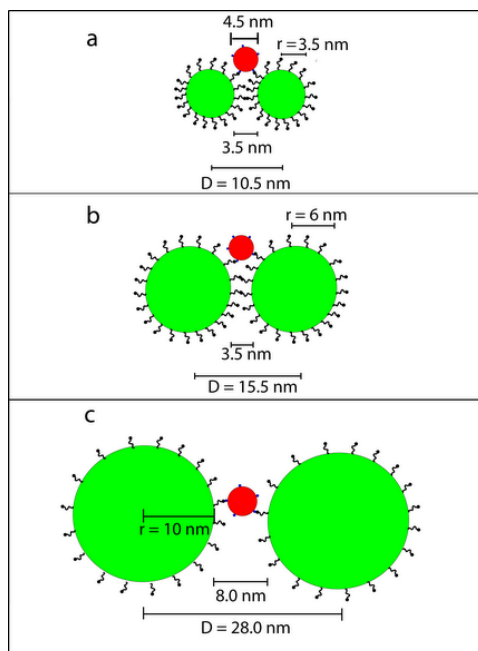


Fig. S3 Schematic representations of LTB interaction with (a) Gal-gAuNP-7, (b) Gal-gAuNP-12, and (c) Gal-gAuNP-20.

The observation that Gal-gAuNP-12 is more effective at detecting LTB than either Gal-gAuNP-7 or Gal-gAuNP-20 may possibly be explained by consideration of the dependence of inter-

particle plasmon coupling on both the size of the AuNPs and the inter-particle distances between AuNPs in the aggregates. This dependency can be quantitatively expressed by the term $D/(2r)$, where D is the distance between the centres of adjacent particles, and $2r$ is the particle diameter. Previous studies have shown that strong interparticle plasmon coupling between adjacent particles occurs when $D/(2r)$ is less than 1.2. In the case of **Gal-gAuNP-7**, since the length of the ligand on the surface of the particles is approximately 1.75 nm (a figure estimated by assuming an extended conformation for the triethylene glycol linker and a 4C_1 conformation for galactose, see Fig. S2), then the minimum distance between the metal cores when two particles are attached to each other is 10.5 nm, as shown in Fig. S3a. Hence the $D/(2r)$ value for this system is 1.5. However, it should be noted that since aggregated nanoparticles have been reported to show near-field coupling even with $D/(2r)$ values that are greater than 1.2, due to the collective interaction between multiple adjacent nanoparticles, then surface plasmon coupling is nonetheless expected to occur even with a $(D/2r)$ value of 1.5. Similarly, the D value for **Gal-gAuNP-12** is 15.5 (Fig. S3b), and the value of $D/(2r)$ is 1.3. As the $D/(2r)$ value is lower for **Gal-gAuNP-12** than for **Gal-gAuNP-7**, it is therefore expected that surface plasmon coupling should be stronger for **Gal-gAuNP-12** than for **Gal-gAuNP-7**. However, when the size of the Gal-gAuNPs is increased 20 nm, the Gal-gAuNPs may then perhaps preferentially bind to non-adjacent receptor sites on LTB due to the steric hindrance arising from the larger size of the particles. If this were to be the case, it would result in an increase in the $D/(2r)$ value to 1.4 (Fig. S3c), and would provide an hypothetical explanation for the decreased SPR coupling between particles that was observed for **Gal-gAuNP-20** as compared to **Gal-gAuNP-12**.

References

1. M. L. Wolfrom, A. Thompson and M. Inatome, *J. Am. Chem. Soc.*, 1957, **79**, 3868-3871.
2. Z. Liu, H.-S. Byun and R. Bittman, *Org. Lett.*, 2010, **12**, 2974-2977.
3. R. Mukthavaram, S. Marepally, M. Y. Venkata, G. N. Vegi, R. Sistla and A. Chaudhuri, *Biomater.*, 2009, **30**, 2369-2384.
4. C. L. Schofield, B. Mukhopadhyay, S. M. Hardy, M. B. McDonnell, R. A. Field and D. A. Russell, *Analyst*, 2008, **133**, 626-634.
5. J. M. de la Fuente, A. G. Barrientos, T. C. Rojas, J. Rojo, J. Cañada, A. Fernández and S. Penadés, *Angew. Chem. Int. Ed.*, 2001, **40**, 2257-2261.
6. Á. G. Barrientos, J. M. De la Fuente, T. C. Rojas, A. Fernández and S. Penadés, *Chem. - Eur. J.*, 2003, **9**, 1909-1921.

7. S. K. Sivaraman, S. Kumar and V. Santhanam, *J. Colloid Interface Sci.*, 2011, **361**, 543-547.
8. G. Frens, *Nature Phys. Sci.*, 1973, **241**, 20.